

NO-A189 291

A POLARIZATION DIVERSITY METEOROLOGICAL RADAR SYSTEM

1/1

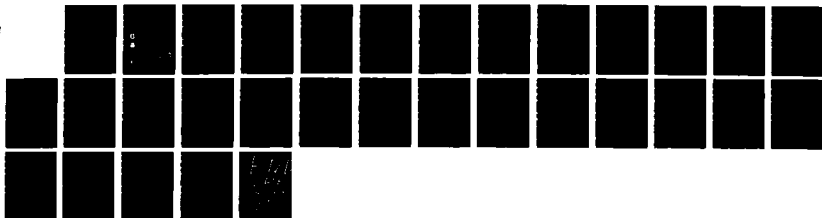
(U) AIR FORCE GEOPHYSICS LAB HANSCOM AFB MA

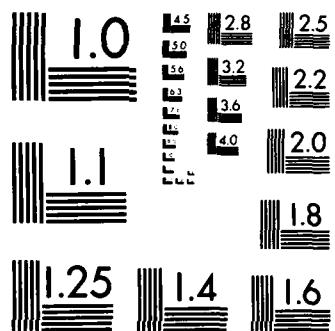
J I METCALF ET AL 19 MAR 87 AFGL-TR-87-0105

UNCLASSIFIED

F/G 17/9

ML





MICROCOPY RESOLUTION TEST CHART
NATIONAL BUREAU OF STANDARDS-1963-A

AD-A189 291

DTIC FILE COPY

④

AFGL-TR-87-0105

INSTRUMENTATION PAPERS, NO. 333

A Polarization Diversity Meteorological Radar System

JAMES I. METCALF

GRAHAM M. ARMSTRONG

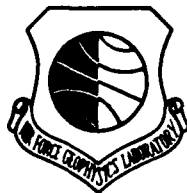
ALEXANDER W. BISHOP



19 March 1987



Approved for public release; distribution unlimited.



DTIC
ELECTE
DEC 1 0 1987
S E D

ATMOSPHERIC SCIENCES DIVISION

PROJECT 6670

AIR FORCE GEOPHYSICS LABORATORY

HANSCOM AFB, MA 01731

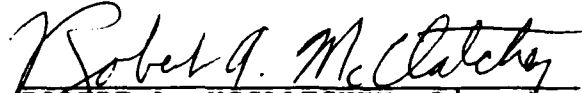
87 1 1

"This technical report has been reviewed and is approved for publication"

FOR THE COMMANDER



KENNETH M. GLOVER, Chief
Ground Based Remote Sensing Branch
Atmospheric Sciences Division



ROBERT A. MCCLATCHEY, Director
Atmospheric Sciences Division

This document has been reviewed by the ESD Public Affairs Office (PA) and is releasable to the National Technical Information Service (NTIS).

Qualified requestors may obtain additional copies from the Defense Technical Information Center. All others should apply to the National Technical Information Service.

If your address has changed, or if you wish to be removed from the mailing list, or if the addressee is no longer employed by your organization, please notify AFGL/DAA, Hanscom AFB, MA 01731. This will assist us in maintaining a current mailing list.

Unclassified

SECURITY CLASSIFICATION OF THIS PAGE

REPORT DOCUMENTATION PAGE				Form Approved OMB No. 0704-0188	
1a. REPORT SECURITY CLASSIFICATION Unclassified			1b. RESTRICTIVE MARKINGS		
2a. SECURITY CLASSIFICATION AUTHORITY			3. DISTRIBUTION/AVAILABILITY OF REPORT		
2b. DECLASSIFICATION/DOWNGRADING SCHEDULE			Approved for Public Release; Distribution Unlimited		
4. PERFORMING ORGANIZATION REPORT NUMBER(S) AFGL-TR-87-0105 IP, No. 333			5. MONITORING ORGANIZATION REPORT NUMBER(S)		
6a. NAME OF PERFORMING ORGANIZATION Air Force Geophysics Laboratory		6b. OFFICE SYMBOL (If applicable) LY	7a. NAME OF MONITORING ORGANIZATION		
6c. ADDRESS (City, State, and ZIP Code) Hanscom AFB Massachusetts, 01731-5000			7b. ADDRESS (City, State, and ZIP Code)		
8a. NAME OF FUNDING/SPONSORING ORGANIZATION		8b. OFFICE SYMBOL (If applicable)	9. PROCUREMENT INSTRUMENT IDENTIFICATION NUMBER		
8c. ADDRESS (City, State, and ZIP Code)			10. SOURCE OF FUNDING NUMBERS		
PROGRAM ELEMENT NO. 62101F		PROJECT NO. 6670	TASK NO. 16	WORK UNIT ACCESSION NO. 03	
11. TITLE (Include Security Classification) A Polarization Diversity Meteorological Radar System (U)					
12. PERSONAL AUTHOR(S) Metcalf, James I., Armstrong, Graham M., Bishop, Alexander W.					
13a. TYPE OF REPORT Scientific Interim		13b. TIME COVERED FROM _____ TO _____	14. DATE OF REPORT (Year, Month, Day) 1987 March 19		15. PAGE COUNT 32
16. SUPPLEMENTARY NOTATION					
17. COSATI CODES			18. SUBJECT TERMS (Continue on reverse if necessary and identify by block number)		
FIELD	GROUP	SUB-GROUP	Polarization diversity weather radar , Dual polarization radar , Polarization switching ,		
19. ABSTRACT (Continue on reverse if necessary and identify by block number) The AFGL 10-cm Doppler weather radar was modified to enable the measurement of the differential reflectivity between horizontal and vertical polarizations in addition to the absolute reflectivity and the Doppler mean velocity and spectrum variance. Polarization switching is achieved by means of a diplexer, which separates at the antenna the transmitted signals of two frequencies, 2710 and 2760 MHz, and permits nearly simultaneous transmission of signals of orthogonal polarizations. Signals of these frequencies can be transmitted either with horizontal and vertical polarization, respectively, or with left and right circular polarization, respectively. We describe the design and performance of the diplexer and the performance of the real-time data processor, present examples of meteorological measurements, and discuss future developments of the radar system.					
20. DISTRIBUTION/AVAILABILITY OF ABSTRACT <input type="checkbox"/> UNCLASSIFIED//UNLIMITED <input checked="" type="checkbox"/> SAME AS RPT <input type="checkbox"/> DTIC USERS			21. ABSTRACT SECURITY CLASSIFICATION Unclassified		
22a. NAME OF RESPONSIBLE INDIVIDUAL James Metcalf			22b. TELEPHONE (Include Area Code) (617) 377-4405		22c. OFFICE SYMBOL LY

Preface

We gratefully acknowledge the efforts of our technicians, TSgt Richard Chanley, A1C Gregory Potter, Edward Duquette, Ruben Novack, and William Smith, in the construction and testing of the data processor; the construction, testing, and installation of the microwave diplexer; and the acquisition and processing of the data. 1Lt Paul Sadoski and Pio Petrocchi aided in the data acquisition. We are indebted to Ralph Donaldson, Jr., of ST Systems Corp., and to Frank Ruggiero of AFGL (formerly of ST Systems Corp.) for providing the Doppler wind analysis program and guidance in using it. We are especially indebted to Paul Desrochers of ST Sytems Corp. for providing and modifying the program used to generate the B-scan displays of absolute and differential reflectivity and providing guidance in its use.



Accession For	
NTIS GRA&I	<input checked="" type="checkbox"/>
DTIC TAB	<input type="checkbox"/>
Unannounced	<input type="checkbox"/>
Justification	
By	
Distribution/	
Availability Codes	
Avail and/or	
Dist	Special
A-1	

Contents

1. INTRODUCTION	1
2. MICROWAVE DIPLEXER AND MECHANICAL SWITCHES	3
3. RECEIVER	7
4. DATA PROCESSOR	7
4.1 Reflectivity and Differential Reflectivity	7
4.2 Doppler Mean Velocity and Spectrum Variance	12
5. MEASUREMENTS	13
5.1 Weather Situation	13
5.2 Absolute Reflectivity	13
5.3 Differential Reflectivity	16
5.4 Doppler Mean Velocity	19
5.5 Evaluation	19
6. FUTURE DEVELOPMENTS	22
6.1 Multi-Channel Receiver	22
6.2 High-Power Microwave Switch	22
6.3 Processor Modifications	23
6.4 Antenna Measurements	23
REFERENCES	25

Illustration

1. Schematic Diagram of the Radar System	2
2. Diplexer Isolation as a Function of Pressure in the Waveguide	4
3. Processor Output Calibration for the 2710 MHz Channel	9
4. Processor Output Calibration for the 2760 MHz Channel	10
5. Reflectivity at 4.5° Elevation, 90-150° Azimuth, and 16-35 km Range	14
6. Reflectivity at 5.5° Elevation, 90-150° Azimuth, and 11-30 km Range	15
7. Differential Reflectivity Corresponding to Figure 5	17
8. Differential Reflectivity Corresponding to Figure 6	18
9. Wind Sounding Derived From Radar Observations	20
10. Wind Sounding by National Weather Service Rawinsonde	20
11. Doppler Velocity Measured at 1.5° Elevation Angle and 46 km Range	21
12. Doppler Velocity Measured at 2.5° Elevation Angle and 28 km Range	21

Tables

1. Antenna and Diplexer Calibration Measurements	5
2. Processor Calibration Parameters	12

A Polarization Diversity Meteorological Radar System

1. INTRODUCTION

The 10-cm Doppler weather radar operated by AFGL at Sudbury, Mass., has undergone a series of modifications to enable the measurement of polarization dependent parameters of backscattered signals. The original design of the radar and the design of the new or modified components have been described in a series of reports.^{1,2,3,4} Implementation of antenna modifications has also been reported.⁵

Having achieved the intermediate goal of measuring the differential reflectivity between horizontally and vertically polarized signals, we present here a descrip-

(Received for publication 16 March 1987)

1. Bishop, A.W., and Armstrong, G.M. (1982) A 10 cm Dual Frequency Doppler Weather Radar, Part I: The Radar System, AFGL-TR-82-0321 (I), AD A125885.
2. Ussailis, J.S., Leiker, L. A., Goodman, R.M., IV, and Metcalf, J.I. (1982) Analysis of a Polarization Diversity Weather Radar Design, AFGL-TR-82-0234, AD A121666.
3. Armstrong, G.M., and Metcalf, J.I. (1983) A Polarization Diversity Radar Data Processor, AFGL-TR-83-0111, AD A134011.
4. Bishop, A.W., and Metcalf, J.I. (1985) A Multi-Channel Radar Receiver, AFGL-TR-85-0006, AD A156058.
5. Ussailis, J.S., and Bassett, H.L. (1984) Polarization Diversity Addition to the 10 Centimeter Doppler Weather Radar, AFGL-TR-84-0239, AD A156062.

tion of the system and some examples of the measurement capability of the modified radar. The present radar system configuration is shown schematically in Figure 1. The principal components discussed in this report are the diplexer and mechanical switches behind the antenna, the receivers, and the data processor. The radar was used to observe precipitation and velocity structure in several storms during the late fall and winter of 1986-1987; one of these yielded the data presented in this report. We conclude with a survey of anticipated further modifications that will expand the measurement capability.

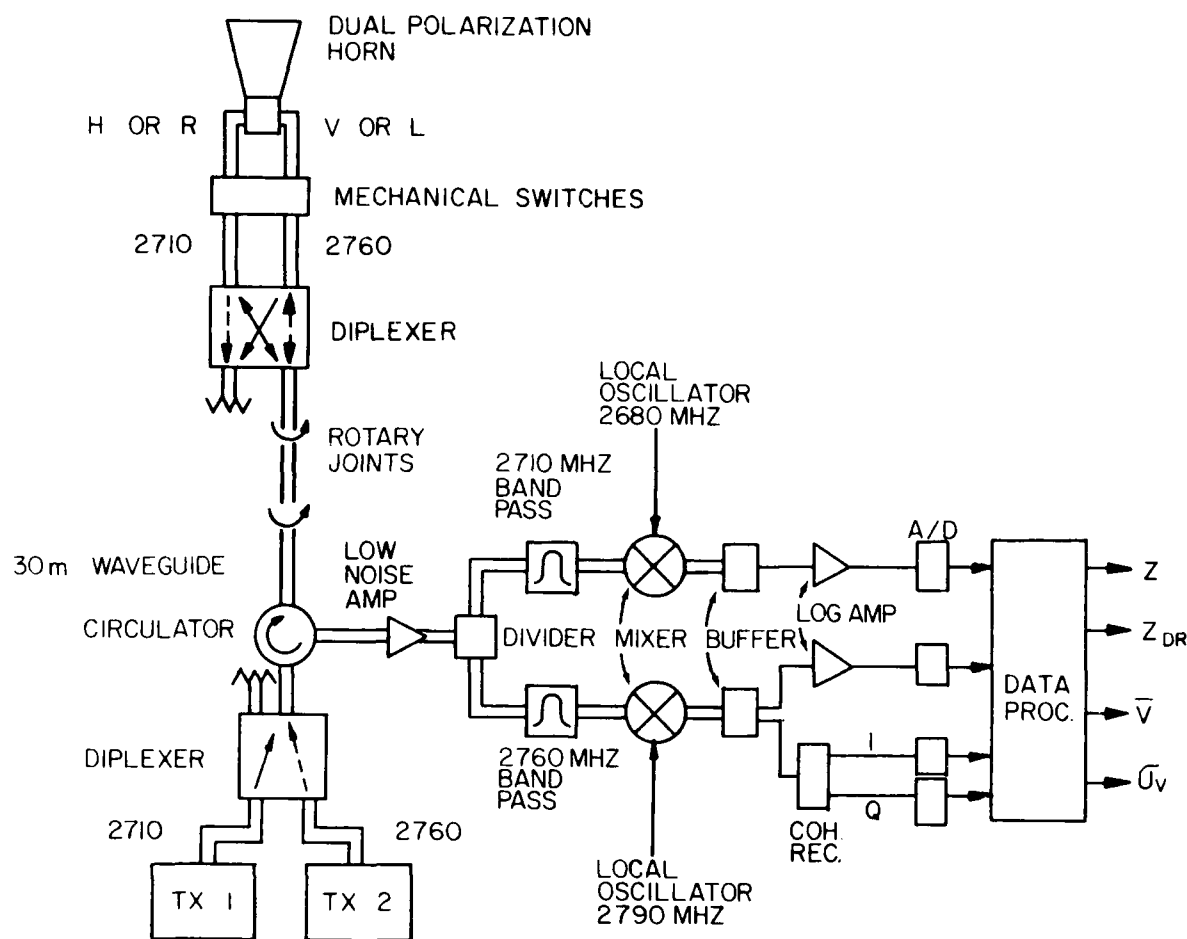


Figure 1. Schematic Diagram of the Radar System. Key elements discussed in this report are the diplexer, polarizer assembly, dual logarithmic receivers, and data processor

2. MICROWAVE DIPLEXER AND MECHANICAL SWITCHES

The modification plan specified the switching of the transmitted signal between orthogonal polarizations on successive pulses, to optimize the measurement of differential reflectivity. Our plan is to switch polarizations by means of an electronically controlled device conceptually similar to those used in other meteorological research radars. Delays in the acquisition of a high-power microwave switch led us to consider and implement an alternative approach, utilizing the dual-frequency capability of the original radar system. Two transmitters generate pulsed signals of 2710 and 2760 MHz, respectively, which are combined in a single waveguide by a diplexer.¹ This diplexer prevents the reflection of either signal into the other transmitter. We constructed a second diplexer and installed it behind the antenna, to separate the two transmitted frequencies at that point. The signals are then fed into the respective input ports of the polarizer assembly. Depending on the setting of two mechanical switches between the diplexer and the polarizer, a signal of 2710 MHz is transmitted with either horizontal or left circular polarization, while a signal of 2760 MHz is transmitted with either vertical or right circular polarization. Signals of orthogonal polarizations, either vertical and horizontal or right and left circular, can be transmitted nearly simultaneously by the two transmitters. The transmitted pulses are offset by 2 μ sec so that the two high-power signals are not present simultaneously in the waveguide. This offset eliminates intermodulation products and reduces the pressure required in the waveguide.

High isolation between the diplexer output ports is critical to the accurate measurement of polarization-dependent parameters. The isolation is strictly determined by the linear dimensions of the device, which establish the phase relations of signals of the two frequencies at the outputs. Within the device, the signals are divided in a hybrid, passed through separate waveguide paths, and recombined through a second hybrid so that signals of the two frequencies recombine in phase at one output port and out of phase at the other port and vice versa. Prior to installation, we tuned the device to achieve maximum isolations of 32 and 34 dB at 2710 and 2760 MHz, respectively. In other words, an input frequency of 2710 MHz, for example, yields an output signal at the nominal 2760 MHz output port, which is 32 dB below the output signal at the nominal 2710 MHz output port. We normally operate the radar with 10 psi pressure of dry nitrogen in the waveguide to prevent arcing. Distortion of the waveguides of the diplexer under pressure seriously degraded the isolation, but we almost eliminated this effect by clamping the waveguide and adjusting the clamps to obtain optimum isolation. The clamp arrangement was necessary because the tuning adjustments had to be sealed before the waveguide was pressurized. The variation of isolation with gas pressure in the waveguide is shown in Figure 2. The degraded performance at zero pressure is

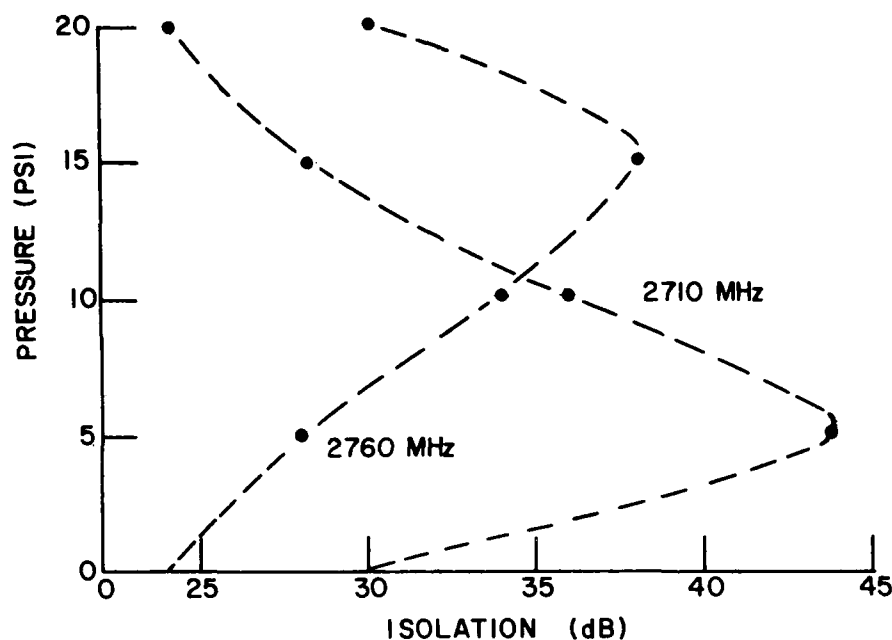


Figure 2. Diplexer Isolation as a Function of Pressure in the Waveguide. Isolation, measured at each frequency, is the logarithmic difference of power between the output ports. Measurements at 2710 and 2760 MHz reveal joint optimization near 11 psi. Clamps used to achieve maximum isolation near 10 psi introduce residual distortion of waveguide, which degrades isolation at zero pressure

due to residual distortion of the waveguide by the clamps. The voltage standing wave ratio (VSWR) of the diplexer is 1.133 at 2710 MHz and 1.123 at 2760 MHz, measured at the input port with the output ports terminated by loads each having a VSWR less than 1.02. The VSWR of the assembled diplexer, mechanical switch assembly, polarizer, and horn is 1.225 at 2710 MHz and 1.035 at 2760 MHz. The VSWR measured near the transmitters, using a directional coupler to sample the transmitted and reflected signals, is 1.183 at 2710 MHz; attenuation of about 2 dB in the waveguide accounts for the lower VSWR.

The linear polarization characteristics of the radar system were measured approximately by means of a standard gain horn at Nobscot Hill in Framingham, MA, 7.9 km south-southeast of the radar. The measurements, other pertinent parameters, and derived quantities are summarized in Table 1. The quantity described as "radar gain" represents the combined gain of the radar antenna (one-way, on-axis) and loss in the radar microwave components. The one-way, on-axis differential gain of the radar, defined by $10 \log(G_H) - 10 \log(G_V)$, is -0.65 dB. The two-way differential gain, equal to twice this value, is used to correct the estimate of differential reflectivity derived from the processor (see Section 4). The cross-

Table 1. Antenna and Diplexer Calibration Measurements

Frequency (MHz)	2710	2760
Transmitted power (dBm)	8.85	5.88
Gain of transmit horn (dB)	15.15	15.26
Path loss (dB)	119.55	119.72
Received power (dBm)		
Horizontal polarization	-56.42	-88.5
Vertical polarization	-80.2	-58.8
Radar Gain (Co-polar, dB)	39.13	39.78
Cross-polarization ratio (dB)	23.78	29.70

polarized received signals, that is, the 2710 MHz signal when the transmitted signal is vertically polarized and the 2760 MHz signal is horizontally polarized, are also listed in Table 1. The resulting cross-polarization ratios are probably of limited value for characterizing the polarization performance of the radar antenna, as the radar beam axis is theoretically a cross-polarization null.

Because the hybrids in the diplexer are not perfect, the diplexer may yield higher output isolation at frequencies slightly different from the nominal design frequencies. We tested this characteristic of the diplexer by tuning it to maximum isolation (61 dB) at 2710 MHz, then varying the other frequency to achieve the complementary maximum isolation. We found a maximum isolation of 61 dB at 2761.22 MHz and isolation of 36 dB or better within ± 500 kHz of this frequency, that is, for a 1 MHz bandwidth.

The diplexer offers several advantages for dual polarization transmission.

- (1) It requires no controls, as it is a passive device.
- (2) It presents negligible signal loss, as it is constructed of unobstructed waveguide components.
- (3) It permits nearly simultaneous transmission of orthogonally polarized signals.
- (4) Doppler velocity estimates are derived from received signals of fixed polarization, eliminating any biases due to differential backscatter amplitude, propagation differential phase shift, or differential attenuation.

However, there are corresponding disadvantages.

(1) Backscattered signals of the two frequencies are statistically independent. Hence, the differential reflectivity is measurable with a standard error of estimate of 0.7 to 0.9 dB at best, rather than the 0.1 to 0.2 dB error achievable from highly correlated successive samples with horizontal and vertical polarizations at a single frequency.⁶

(2) Backscattered signals of either frequency having polarization orthogonal to the respective transmitted polarization cannot be received through the diplexer. This limitation is discussed in the following paragraph.

(3) Differences in antenna patterns and in polarization errors between the two frequencies may adversely affect the measurements. In the future, we shall try to optimize antenna characteristics jointly at the two frequencies.

The present configuration of the system permits the reception of only the co-polarized signals of each frequency. The polarizer feeds the orthogonally polarized backscatter signal of each frequency into the diplexer port corresponding to the other frequency. These orthogonally polarized signals are recombined at the fourth port of the diplexer, which is terminated as shown in Figure 1. When the mechanical switches are set for linear polarization, the "main" backscattered signal is received in each receiver channel. When the mechanical switches are set for circular polarization, only the "depolarized" backscattered signals (due to non-spherical scatterers) are received, because the polarizations of the "main" backscattered signals are orthogonal to those of the respective transmitted signals. By switching between the linear and circular mode, we can derive a measurement of the cancellation ratio, as defined by Offutt⁷ and by Newell et al.,⁸ which can be related to the circular depolarization ratio. The exact relationship is dependent on the particle size and shape distributions. The setting of the mechanical switches can be changed within a few tenths of a second, but these switches are not intended for frequent repeated operation during extended periods of time. In practice, we expect to hold them at a given setting for extended periods during radar operations.

6. Bringi, V.N., Seliga, T.A., and Cherry, S.M. (1983) Statistical properties of the dual-polarization differential reflectivity (Z_{DR}) radar signal, IEEE Trans. Geosci. and Remote Sens. GE-21:215-220.

7. Offutt, W.B. (1955) A review of circular polarization as a means of precipitation clutter suppression and examples, Proc. Natl. Electron. Conf. 11:94-100.

8. Newell, R.E., Geotis, S.G., and Fleisher, A. (1957) The Shape of Rain and Snow at Microwavelengths, Res. Rept. 28, Dept. of Meteorology, Mass. Inst. of Tech.

3. RECEIVER

The multi-channel receiver described by Bishop and Metcalf⁴ has been constructed but has not yet been installed. Its installation will require the installation of two circulators between the diplexer and the mechanical switch assembly behind the antenna and the installation of new multi-channel rotary joints in the antenna mount to carry the signals of each received polarization separately. The signals in each polarization channel are to be separated by frequency in the multi-channel receiver.

As an interim configuration, we have installed matched logarithmic receivers on the two receiver channels, so that power measurements can now be made over a wide dynamic range at both frequencies. Because the horizontally polarized 2710 MHz signal is used for absolute reflectivity measurement, the Doppler mean velocity and spectrum variance are derived from the 2760 MHz channel. This use of the two frequencies is the inverse of their use in the original system.

4. DATA PROCESSOR

4.1 Reflectivity and Differential Reflectivity

The data processor was constructed in general accordance with the design presented by Armstrong and Metcalf.³ Several details of timing and data flow were changed to accommodate the microwave diplexer. Logarithmic power outputs from both receiver channels are now sampled concurrently at 1024 ranges from the radar, but with a 2- μ sec delay on the 2760 MHz channel. The original plan was to digitize the logarithmic power output from one channel only, flagging the samples as horizontally or vertically polarized according to the setting of the microwave switch. The parameters of time and range averaging (2 to 1024 pulses by factors of 2; and 1, 2, or 4 range cells) are set as in the original design, but the timing is simplified, as each time average is based on a succession of uniformly spaced samples. Correcting an error in the original design, we perform all averaging before reconvertng to logarithmic values.

Within the processor, numbers proportional to the received power are derived from two sets of programmable read-only memories (PROMs), one set for each frequency channel. These numbers, each comprising an 11-bit mantissa and a 5-bit exponent (base 2), span a dynamic range of 2^{32} (nominally from 0.5×2^0 to 0.999×2^{31}) and are calculated for each input bit count on the basis of the calibrations of the respective receivers and analog-to-digital (A/D) converters. The logarithmic part of each calibration curve is defined by an equation of the form

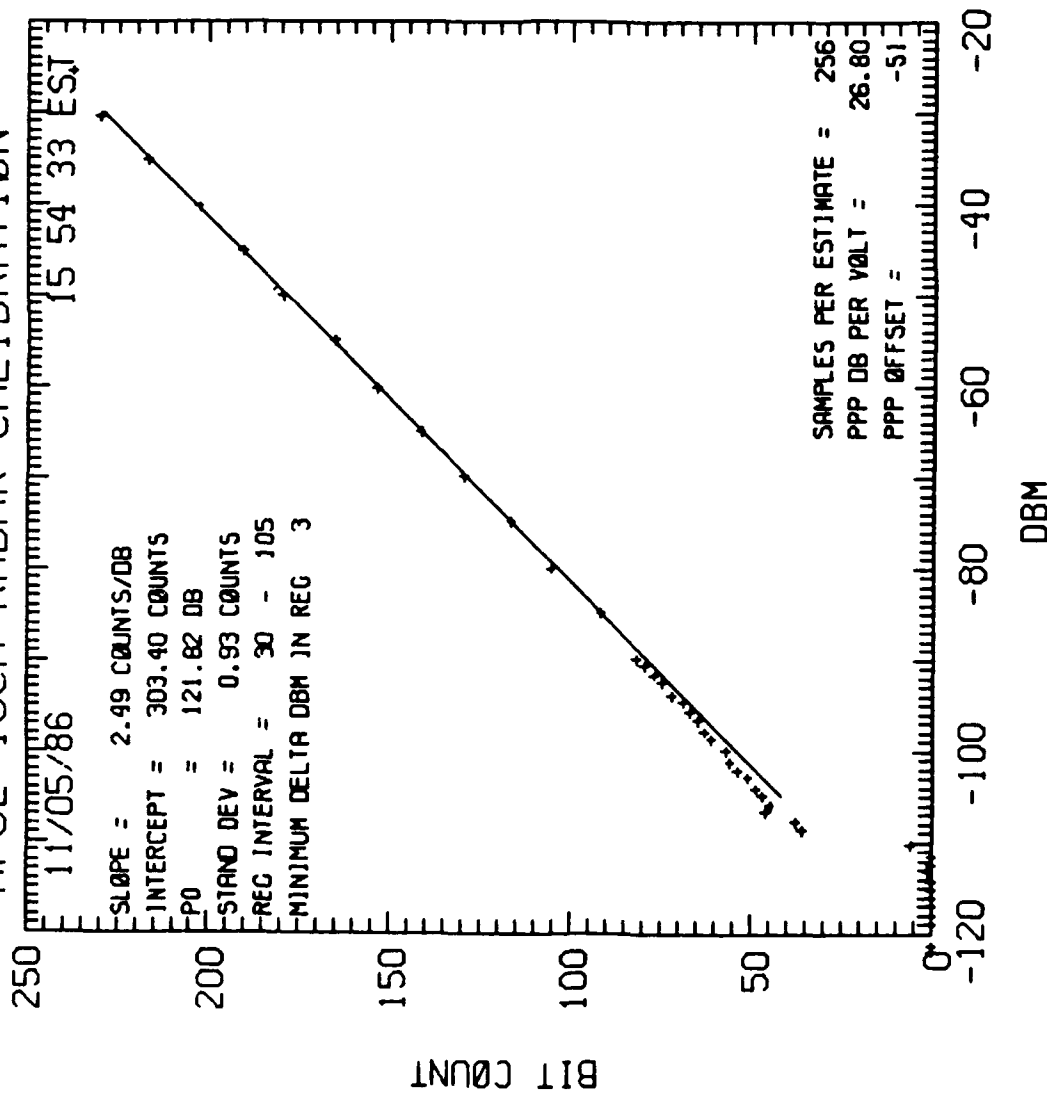
$$I = I(0) + S \cdot 10 \log P \quad (1)$$

where I is the bit count from the A/D converter, $I(0)$ the intercept, S the slope in bit counts per decibel, and $10 \log P$ the power in decibels relative to 1 milliwatt (dBm).

Determining these calibration curves presents some difficulties, particularly near the noise level, due to fluctuations of the receiver output signals. If either of these calibrations is determined to have changed for any reason, a new set of PROMs can be programmed to replace the original set. After the averaging is completed, the power is reconverted to a 10-bit logarithmic value on a fixed scale of 30 bit counts per factor of 2 (9.966 bit counts per dB). The difference of the logarithmic values derived from the two channels yields an estimate of the differential reflectivity with about 0.1 dB digital resolution. The eight most significant bits from the 2710 MHz channel are used to derive the absolute reflectivity, with a nominal output calibration of 2.491 bit counts per dB (30 bit counts per factor of 16, yielding 0.4 dB digital resolution). The 8-bit outputs of both frequency channels are available for calibration purposes. Typical output calibrations are shown in Figures 3 and 4. The calibration of each output of the processor should be a straight line in logarithmic coordinates between the minimum detectable signal and the saturation level. Deviations from the straight line at low signal level and deviations from the nominal output slope reflect inaccuracy in determining the correct calibration of the receivers and the A/D converters. Analytically, within the logarithmic domain of the receiver output, the 8-bit processor output corresponds to the quantity $\langle P^{S/2.491} \rangle$, where P is the receiver output power, S is the measured slope of the processor output calibration, and the angled brackets denote a time average. The estimate of averaged received power derived through the processor output calibration thus is equal to $[\langle P^{S/2.491} \rangle]^{2.491/S}$. If $|(S/2.491) - 1| \ll 1$, the resulting bias of the estimated power is given in decibels by $10 \cdot \log(e) \cdot (1 - C) \cdot [(S/2.491) - 1] = 1.84 [(S/2.491) - 1]$, where $C = 0.5772 \dots$ is Euler's Constant, which arises from one of the integrals in the analytical derivation. An early calibration of the processor output yielded $S/2.491 = 1.016$ and 1.012 for the 2710 and 2760 MHz channels, respectively, and a resulting bias of a few hundredths of a decibel in each channel. The current calibration yields $S/2.491 = 1.00$ for each channel.

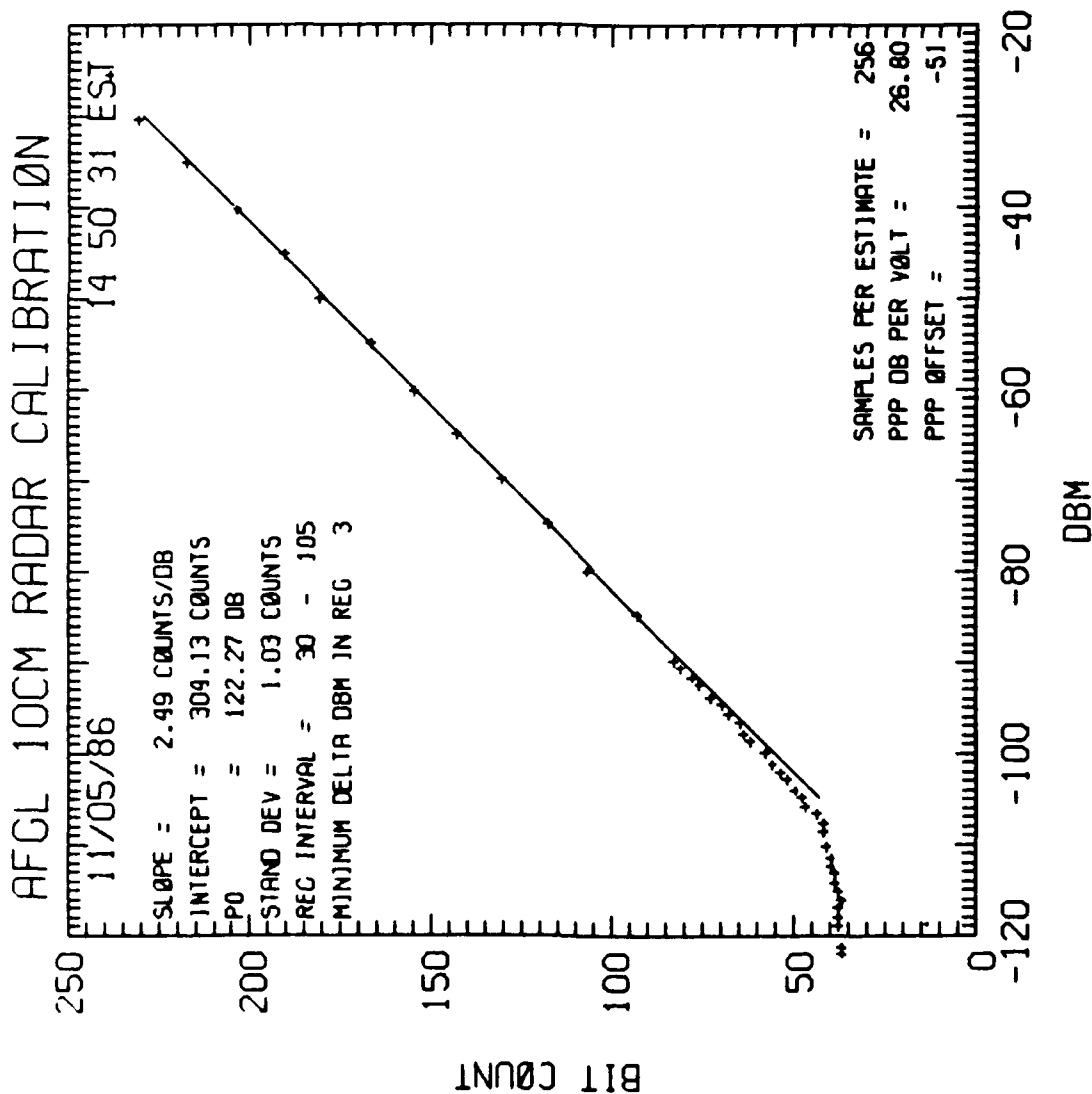
The raw estimate of differential reflectivity in decibels is given by $[I(2710) - I(2760)]/9.966$, where I is the 10-bit processor output. If the calibrations of the input PROMs are not accurate, that is, if the slope of the 8-bit output calibration of either channel differs from 30 bit counts per factor of 16 (2.491 bit

AFGL 10CM RADAR CALIBRATION



BIT COUNT	DBM
238	-75.12
237	-76.90
203	-78.01
191	-79.82
180	-81.80
166	-83.61
154	-85.87
142	-87.88
130	-89.65
117	-91.48
106	-93.66
92	-95.59
82	-97.52
80	-99.30
77	-101.12
72	-103.50
69	-105.38
67	-107.43
65	-109.36
63	-111.49
61	-113.39
56	-115.60
54	-117.88
51	-120.78
49	-122.50
47	-124.67
45	-126.49
43	-128.33
38	-130.30
36	-132.90
0	-134.18
0	-136.06
0	-137.80
0	-139.97
0	-141.79
0	-143.82
0	-146.63
0	-147.73
0	-148.60
0	-150.83
0	-151.67

Figure 3. Processor Output Calibration for the 2710 MHz Channel. Output bit count (8-bit numbers) is shown as a function of power input to the receiver



BIT COUNT	DBM
239	-25.12
231	-27.08
218	-34.90
204	-40.01
191	-44.82
181	-49.80
167	-54.61
155	-59.87
133	-64.68
131	-69.65
118	-74.46
107	-79.56
93	-84.54
83	-89.52
81	-90.30
78	-91.12
73	-93.50
70	-94.38
68	-95.43
64	-96.49
62	-98.39
56	-99.20
54	-100.88
52	-101.78
50	-102.50
48	-103.67
47	-104.99
41	-106.33
42	-107.43
42	-108.30
41	-109.90
40	-111.18
40	-112.06
39	-112.80
38	-113.97
38	-114.79
37	-115.82
36	-116.83
36	-117.73
37	-118.60
37	-120.93
37	-121.67

Figure 4. Processor output calibration for the 2760 MHz Channel. Deviation from straight line at low power implies that input calibration is too steep at low power

counts per dB, then the raw estimate of differential reflectivity becomes:

$$\begin{aligned}
 \frac{[I(2710) - I(2760)]}{9.966} &= \frac{[I_0(2710) - I_0(2760)]}{9.966} \\
 &+ \left[\frac{S(2760)}{2.491} \right] \cdot 10 \log \left[\frac{\langle P(2710) \rangle}{\langle P(2760) \rangle} \right] \\
 &+ \left\{ \frac{[S(2710) - S(2760)]}{2.491} \right\} \cdot 10 \log [\langle P(2710) \rangle] \\
 &+ \left[\frac{S(2760)}{2.491} \right] \cdot 10 \log [P_0(2760)] \\
 &- \left[\frac{S(2710)}{2.491} \right] \cdot 10 \log [P_0(2710)] \\
 &+ \left\{ \frac{[S(2710) - S(2760)]}{2.491} \right\} (1 - C) \cdot 10 \log(e)
 \end{aligned} \tag{2}$$

where P is the received power in milliwatts and I_0 and P_0 are the 10-bit count and received power at which the input and output calibration lines cross. Using the values of these parameters given in Table 2 (based on a processor calibration of 5 November 1986), we determine the differential reflectivity to be:

$$10 \log \left[\frac{\langle P(2710) \rangle}{\langle P(2760) \rangle} \right] = \frac{[I(2710) - I(2760)]}{9.966} + 0.31 \tag{3}$$

The residual correction term is due to the independent calibrations of the two receiver channels at the input to the processor. Prior to calibration, the receivers are adjusted so that the 10-bit outputs of the A/D converters encompass the full dynamic range of the signals and yield a slope of approximately 10 bit counts per dB. The two channels are not constrained to have identical calibrations. Eqs. (2) and (3) are valid if there is no difference in system gain between the two polarizations. The two-way differential gain in decibels, given by

$$\begin{aligned}
 20 \log(G_D) &= 20 [\log(G_H) - \log(G_V)] \\
 &= 20 \left| \log[G(2710)] - \log[G(2760)] \right|
 \end{aligned} \tag{4}$$

Table 2. Processor Calibration Parameters

Signal Frequency (MHz)	2710	2760
Linear polarization	H	V
Input calibration (stored in PROM's):		
Intercept (10-bit)	1216.60	1216.60
Slope (10-bit)	9.72	9.64
Output calibration (5 Nov 86):		
Intercept (8-bit)	303.40	304.13
Slope (8-bit)	2.49	2.49
I_0 (10-bit)	1338	1219
$10 \log(P_0)$ (dBm)	12.50	0.25
S/2.491	1.00	1.00

where G represents one-way gain, must be subtracted from the estimate of differential reflectivity derived from the processor. Thus, for our radar system, using the values shown in Table 1, we have

$$10 \log \left[\frac{\langle P(2710) \rangle}{\langle P(2760) \rangle} \right] = \frac{[I(2710) - I(2760)]}{9.966} + 0.31 + 1.30 \quad (5)$$

4.2 Doppler Mean Velocity and Spectrum Variance

The 2760 MHz signal from which the Doppler parameters are derived is transmitted at a fixed polarization. Hence, a conventional pulse-pair algorithm can be used for computing mean velocity and spectrum variance. Moreover, the 2760 MHz transmitter can be pulsed at a higher rate than the 2710 MHz transmitter, to increase the unambiguous velocity limits, as in the original radar system design. At low elevation angles, the use of a higher pulse repetition rate at 2760 MHz can lead to contamination of the Doppler parameters and differential reflectivity by "second trip" echoes. The presence of such contamination can be deduced easily from displays of the absolute reflectivity, derived from the 2710 MHz channel.

The mean velocity is derived from the phase of the autocovariance function computed at one-pulse lag time. Test signals incorporating a range of frequency shifts have been used to verify the output of the processor and test the display hardware. The spectrum variance is derived from the ratio of the autocovariances

computed at a one-pulse lag and a two-pulse lag, using the formulation of Srivastava et al.⁹ By avoiding use of the zero lag autocovariance in this calculation, we avoid the effect of receiver noise on the Doppler spectrum variance.

5. MEASUREMENTS

5.1 Weather Situation

The first extended operation of the modified radar with the new data processor occurred on 5 and 6 November 1986. A low pressure center developed off the New Jersey coast on 5 November and moved northeastward, passing south of Nantucket in the early morning hours of 6 November and producing widespread precipitation over southern New England. Between 2255 EST on 5 November and 0545 on 6 November, 11.9 mm of rain fell at the radar site, yielding an average rainfall rate of 1.74 mm/hr. The heaviest rainfall occurred at 0247-0258 EST (4.2 mm/hr) and at 0425-0443 (3.4 mm/hr). An additional 2.8 mm of rain fell between 0545 and 1030 on 6 November. The surface temperature throughout the observational period was about 2.5° C, due to a shallow layer of relatively cold air near the surface. The radar was operated from about 2300 EST on 5 November to 0900 on 6 November, predominantly in a volume scan mode. A few elevation scans were performed between 0600 and 0630 and between 0830 and 0900. A strong bright band was detected near 2 km altitude above the radar during the early hours of the precipitation. By 0210 EST, it was detectable mainly in the eastern half of the sky, and, by 0230, it was fading in intensity. A weak bright band was detected during the initial series of elevation scans, but, by the later time, the precipitation had moved to the north and east of the radar and was decreasing in intensity.

5.2 Absolute Reflectivity

Data recorded between 0215 and 0235 EST were selected for detailed analysis and presentation in this report. During this time, the radar was detecting a strong bright band near 2 km altitude above the radar, mainly in the eastern half of the sky. Figures 5 and 6 depict the reflectivity measured in azimuth scans between 90° and 150°. The bright band appeared near 26 km range at 4.5° elevation angle and near 21 km at 5.5° elevation angle. The bright band was somewhat less distinct in the southeast sector than in the northeast, but the variations of differential reflectivity associated with the melting layer were more distinct in the southeast

9. Srivastava, R.C., Jameson, A.R., and Hildebrand, P.H. (1979) Time-domain computation of mean and variance of Doppler spectra, J. Appl. Meteorol. 18:189-194.

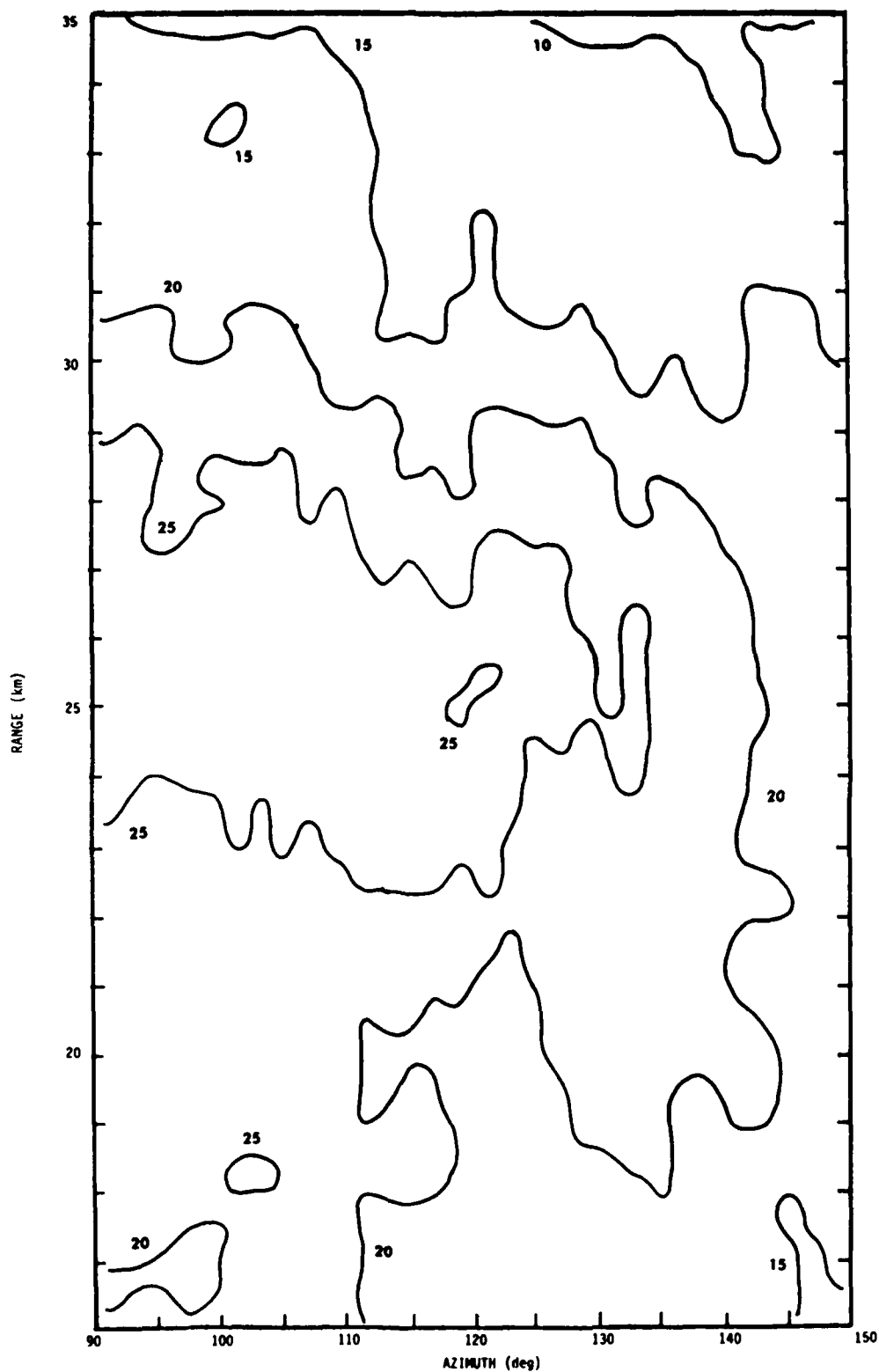


Figure 5. Reflectivity at 4.5° Elevation, 90-150° Azimuth, and 16-35km Range. Original data were averaged over four range cells (600 m). Bright band due to melting layer is evident between 23 and 29 km range

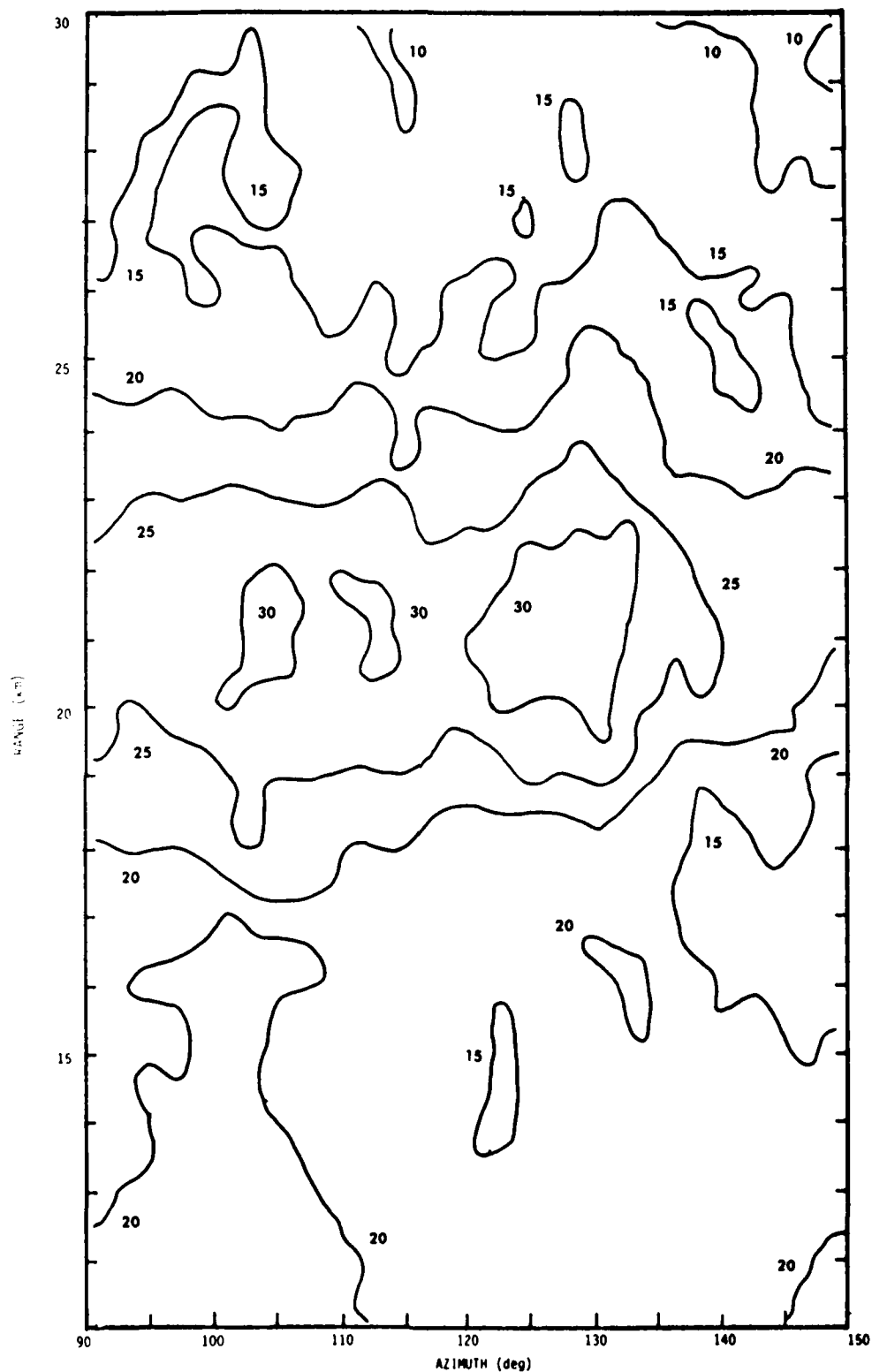


Figure 6. Reflectivity at 5.5° Elevation, 90-150° Azimuth, and 11-30 km Range. Original data were averaged over four range cells (600 m). Bright band is evident between 19 and 24 km range

than in the northeast. The radar reflectivity data were averaged over 256 pulses in the processor, yielding estimates based on approximately 20 independent samples. While this averaging is adequate for the absolute reflectivity, further averaging is necessary to reduce the standard error of the estimate of the differential reflectivity. We used a moving average of variable length in range to process the reflectivity data, so as to reduce the fluctuations of differential reflectivity. The data shown in Figures 5 and 6 were averaged over four range cells (each of 150 m length).

The maximum reflectivity in the bright band is about 34 dBZ at 5.5° elevation angle and about 30 dBZ at 4.5° . This variation is consistent with the increasing vertical extent of the beam with increasing range. The width of the reflectivity maximum, between the 25 dBZ reflectivity contours, is about 5.0 km at 4.5° elevation and 4.0 km at 5.5° , indicating large-scale horizontal uniformity of thickness. There is a marked cellular structure in the bright band, with the rangewise maximum reflectivity varying by 12 dB across this azimuthal domain.

5.3 Differential Reflectivity

Differential reflectivity estimates derived by means of the diplexer appear highly variable, because of their rather high standard error, discussed in Section 3. Figures 7 and 8 depict the differential reflectivity corresponding to Figures 5 and 6. These data are based on reflectivity data averaged over 256 pulses and 8 range cells, because the 4-cell range average yielded unacceptable variability. The estimates of differential reflectivity comprise approximately 160 independent samples and have a standard error of about 0.5 dB.

At each elevation angle, we find a region of maximum differential reflectivity near the height of the bright band. At both 4.5° and 5.5° elevation angle, we find values from 0 to +3 dB above the bright band and -0.5 to +3.5 dB within the bright band. Below the bright band, we find 0 to +1.5 dB at 4.5° elevation angle and 0 to +3 dB at 5.5° . Radar observations recorded elsewhere typically show differential reflectivity values near zero decibels in ice particles above a bright band; the slightly positive values we recorded may be indicative of preferentially oriented ice particles. The maximum differential reflectivity coincident with the bright band is consistent with observations made elsewhere and is generally ascribed to the presence of large, highly-oriented aggregate snow particles in the melting layer. The smaller positive values of differential reflectivity below the bright band are characteristic of small to medium sized raindrops. In the present data, it is difficult to determine whether the small-scale variability is due primarily to statistical fluctuations or to variations of the microphysical characteristics.

An anomaly of differential reflectivity, with strongly negative decibel values,

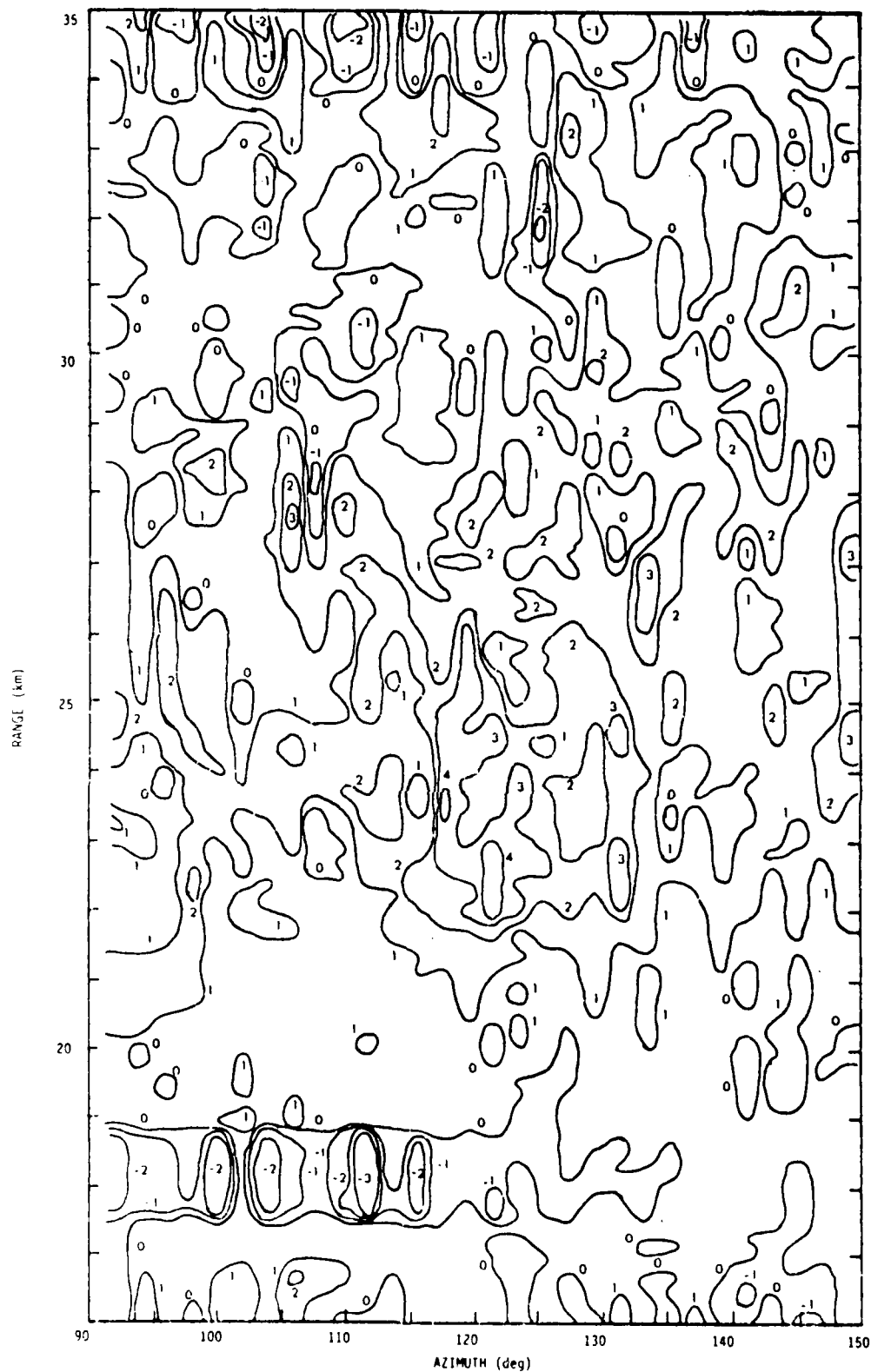


Figure 7. Differential Reflectivity Corresponding to Figure 5. Original data were averaged over eight range cells (1200 m). Large positive values between 22 and 27 km range are associated with the melting layer. Large negative values near 18 km are probably due to a ground target

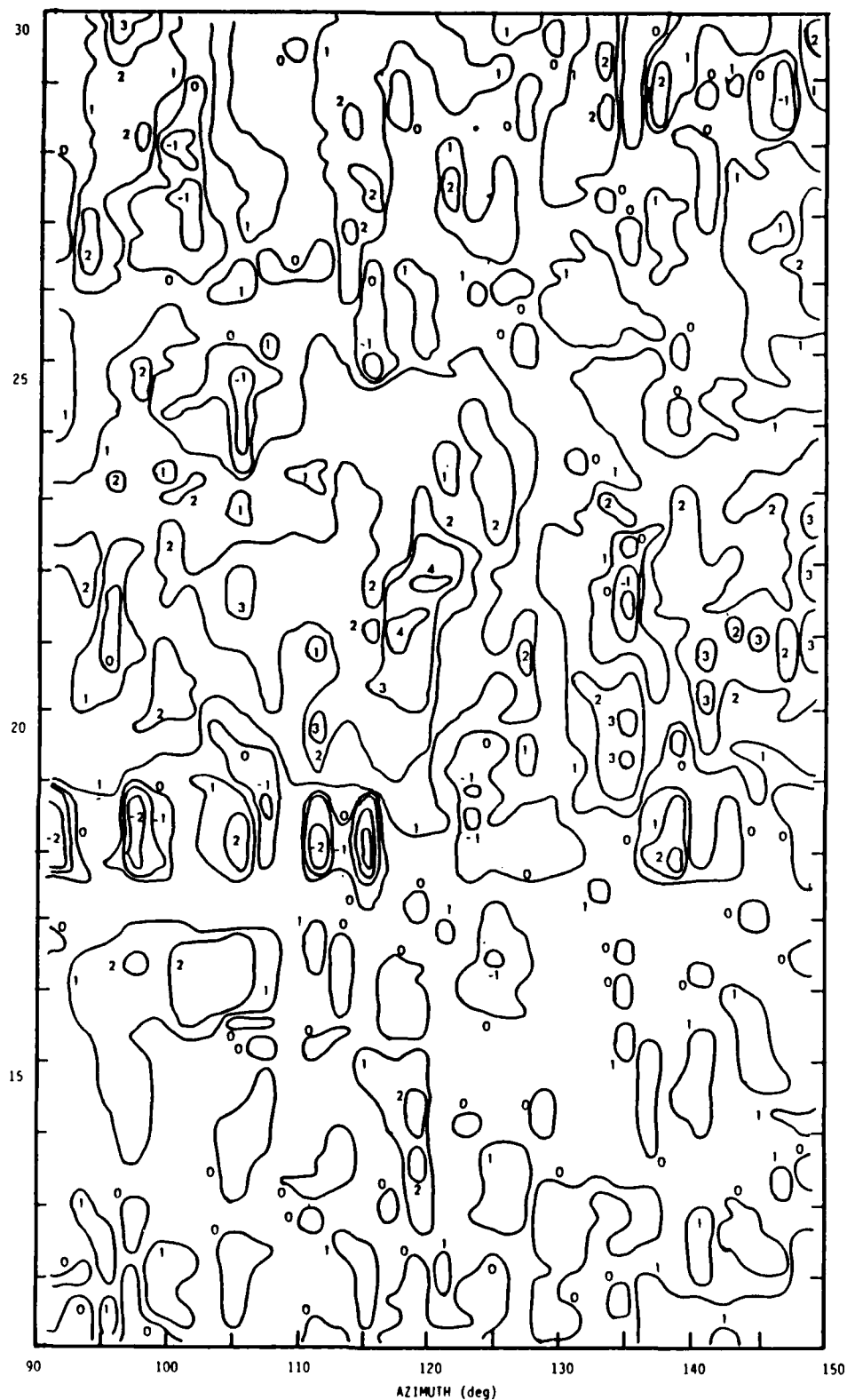


Figure 8. Differential Reflectivity Corresponding to Figure 6. Original data were averaged over eight range cells (1200 m). Large positive values between 19 and 23 km range are associated with the melting layer. Large negative values near 18 km are probably due to a ground target

appears near 18km range at both elevation angles. This is undoubtedly due to a ground target detected in sidelobes. The most likely source of this feature is the group of radio antenna towers on Bear Hill in Waltham, MA, at an azimuth of 101° from the AFGL radar. The tallest of these towers extends to a height of 648 ft (198m) above mean sea level (MSL), which is nearly 100m above the elevation of the radar. Another group of towers, in Needham, MA, extends to more than 1300 ft (400m) MSL, at azimuths of $116-119^\circ$ and ranges of 23-25km. The lack of a similar anomaly of differential reflectivity in this region of the data may be due to the stronger meteorological reflectivity there or to the wider spacing of these towers. The nearly periodic azimuthal variation of differential reflectivity near 35km range in Figure 7 is probably due to the tall buildings of downtown Boston, which are centered about 101° azimuth.

5.4 Doppler Mean Velocity

The Doppler mean velocity estimates generated by the processor were analyzed at several ranges and elevation angles about 0220 EST. The resulting wind profile is shown in Figure 9. The wind profile measured by the National Weather Service at Chatham, MA, at 0700 EST is shown in Figure 10 for comparison. The general features of the wind profile derived from the radar are similar to those of the rawinsonde observation. Both soundings show wind from the east near the surface and rapid veering with height to southwesterly above 2000m MSL. The difference in the wind estimates for 1200m altitude above the radar, derived from 1.5° and 2.5° elevation angles, are due mainly to small-scale wind fluctuations. The variations of the mean Doppler velocity with azimuth at the corresponding elevations and ranges are shown in Figures 11 and 12. The observation at 1.5° elevation and 46km range exhibits periodic fluctuations between 240° and 320° azimuth and a more northerly azimuth of the maximum Doppler velocity than that observed at 2.5° elevation and 28km range. The difference between wind estimates derived at 2.5° and 3.5° elevation angles is much smaller, perhaps due to the weaker shear at 2100m altitude above the radar.

5.5 Evaluation

The measurements reported above and subsequent measurements in similar precipitation systems allow us to offer a preliminary evaluation of the performance of the radar system as a whole and the data processor in particular. The processor, in conjunction with our scan-converter refresh memory displays, yields excellent displays of the absolute reflectivity and the Doppler mean velocity. The design of the new processor remedies a deficiency in our original pulse-pair processor, which has been in use since 1974, in the processing of signals close to the

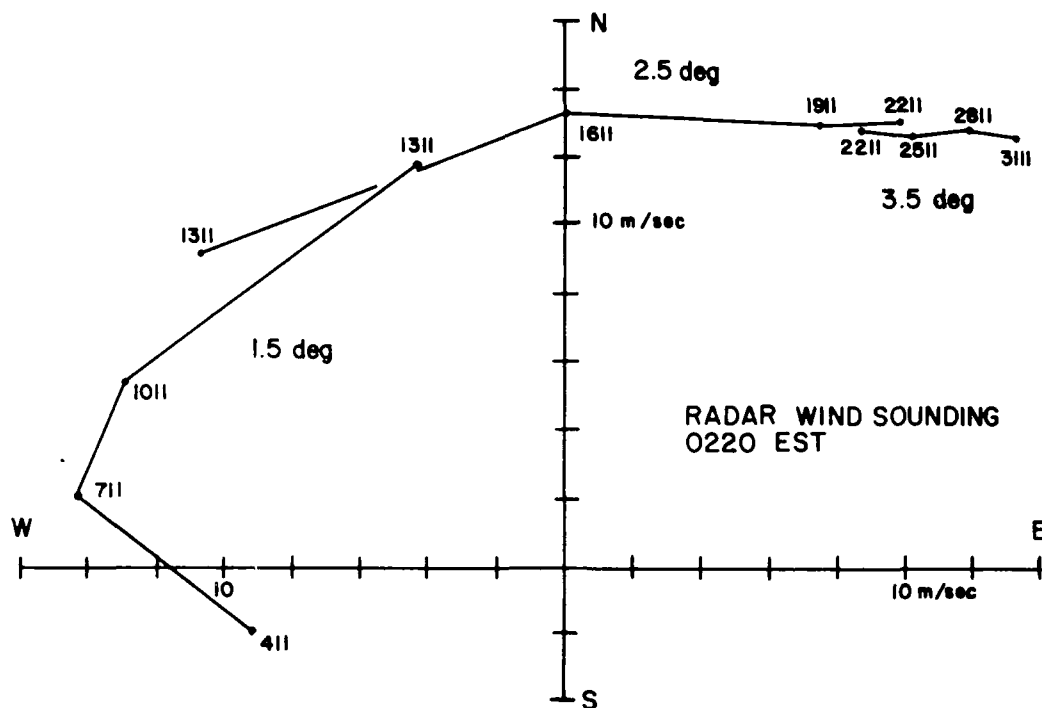


Figure 9. Wind Sounding Derived From Radar Observations. Horizontal wind was computed at intervals of 300m altitude above the radar antenna from measurements about 0220 EST at three elevation angles. Altitudes shown are meters above mean sea level. (The altitude of the antenna is 111m above mean sea level.) Difference between computed winds at 1311m altitude are due to small-scale fluctuations of Doppler velocity

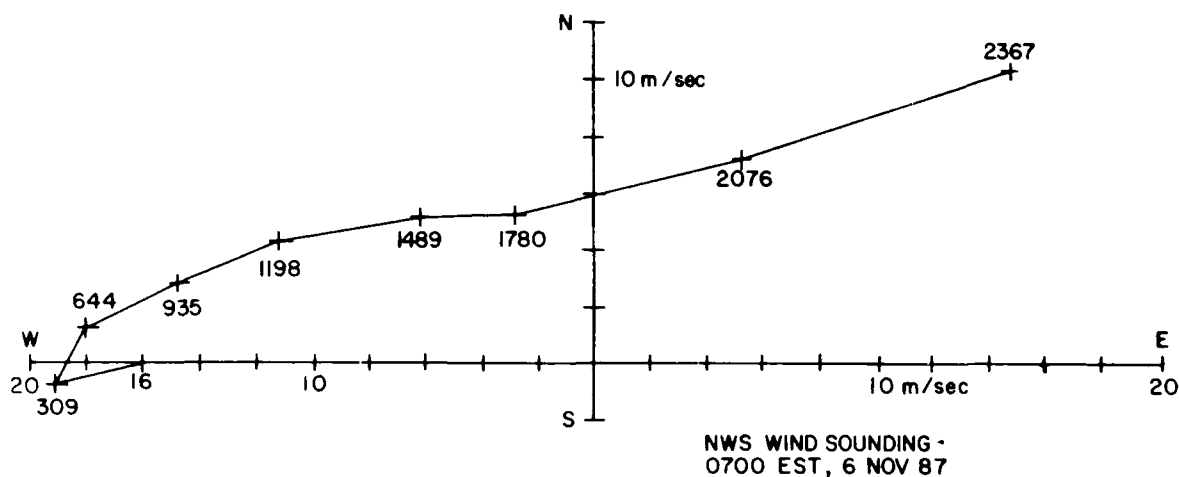


Figure 10. Wind Sounding by National Weather Service Rawinsonde. Sounding was made from Chatham, MA, at 0700 EST (1200 UTC) on 6 November 1986. Altitudes shown are meters above mean sea level. General features compare well with radar observations shown in Figure 9

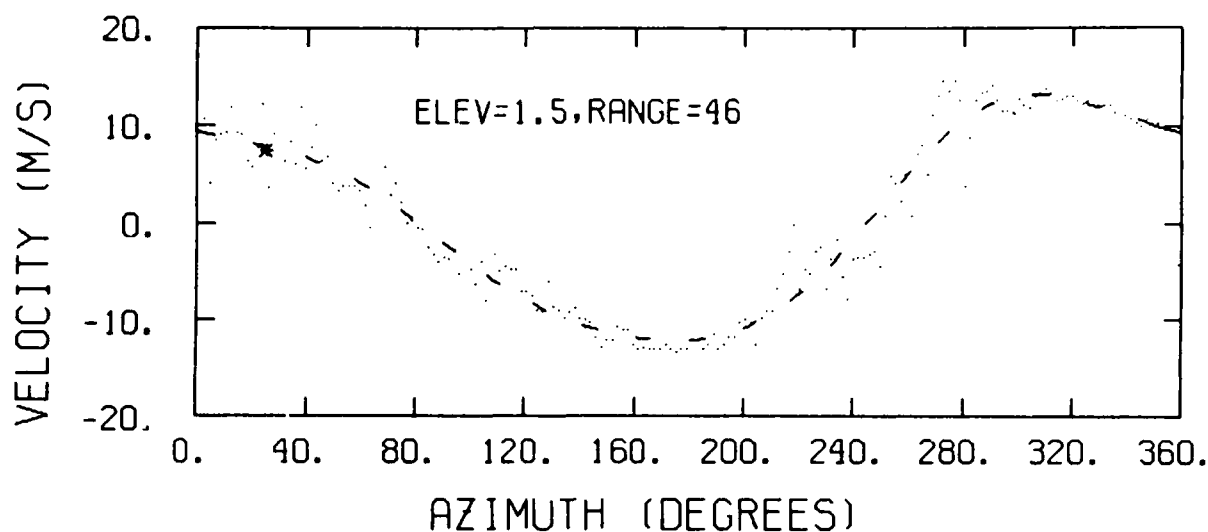


Figure 11. Doppler Velocity Measured at 1.5° Elevation Angle and 46 km Range. Observations correspond to 1200 m altitude above the radar. Small-scale periodic fluctuations are evident between 240° and 320° azimuth

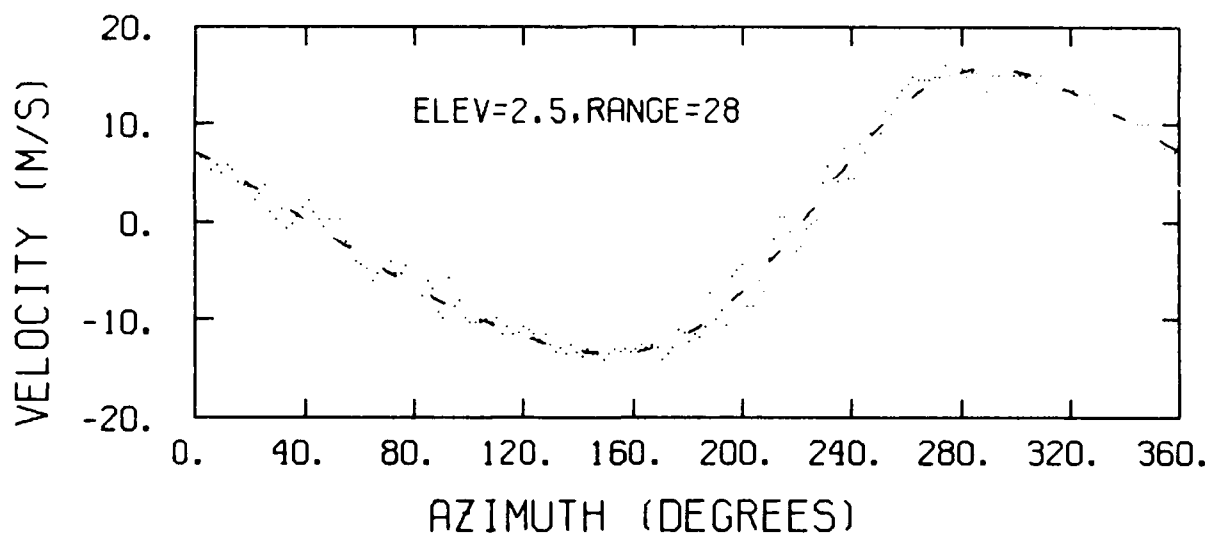


Figure 12. Doppler Velocity Measured at 2.5° Elevation Angle and 28 km Range. Observations correspond to 1200 m altitude above the radar. No small-scale periodic fluctuations of wind are evident in this measurement, but the azimuth of the maximum wind is displaced counterclockwise relative to that shown in Figure 11

receiver noise level. As a result, the new processor yields valid estimates of the Doppler mean velocity over a wider dynamic range of received power than was previously available and generally yields a "cleaner" display of the Doppler mean velocity.

Our initial measurements of polarization differential reflectivity yield results that are quantitatively similar to those observed elsewhere, that is, positive decibel values of small magnitude in rain, larger positive values near the melting level, and decibel values near zero above the melting level, presumably due to ice-phase hydrometeors. Our measurements suffer from a high degree of variability because of the high standard error associated with uncorrelated samples of the horizontal and vertical reflectivities. This variability will be reduced substantially in future measurements, which will utilize the high-power microwave switch.

6. FUTURE DEVELOPMENTS

6.1 Multi-Channel Receiver

Our original plan was to install the receiver in a temperature-controlled enclosure behind the antenna. The resulting 12 video signals (logarithmic power, in-phase amplitude, and quadrature amplitude for each polarization and each frequency) were to be brought through the pedestal by means of slip rings. However, it was determined, following a failure of the azimuth bearing of the pedestal in November 1984, that the bearing would not carry the additional load. Therefore, we acquired new three-channel rotary joints which will carry the transmitted signals through waveguide and the received signals of each polarization in separate coaxial cables. The temperature-controlled enclosure for the receiver is being built on the middle deck of the AB-563/GPS tower on which the antenna is mounted, about 7 m below the antenna. From here, the signals will be carried about 30 m in video cables to the data processor, displays, and recording equipment. We expect to complete the installation this year.

6.2 High-Power Microwave Switch

A high-power switchable circulator built by Raytheon Co. is to replace the diplexer behind the antenna. Its function will be to alternate the transmitted and received polarizations either on a pulse-to-pulse basis or as otherwise required for data processing. It will enable highly accurate measurements of the differential reflectivity and also, in conjunction with the multi-channel receiver, enable simultaneous measurement of the depolarization ratios and cross-correlations corresponding to orthogonal transmitted polarizations. Such measurements will permit us to specify the angular parameters of backscatter and propagation, which are ambiguous in measurements with fixed circular polarization.

The switch was delivered in mid-November 1986. However, because the system as described was already operational at that time, we continued to operate it

in that configuration through February 1987. The new switch is now being installed in anticipation of a series of measurements during April and May 1987.

6.3 Processor Modifications

We are considering several modifications to the data processor. With the installation of the high-power switch, timing is being changed to accommodate the resulting data sequence. More functions may be added after the multi-channel receiver is operational. Initially, we plan to record a subset of the 12 available video signals, according to particular measurement objectives, and to compute depolarization ratios, signal cross-correlations, and differential Doppler velocities between polarization channels in off-line analysis. Calculation of some of these parameters may be incorporated into the data processor if they appear to be valuable for real-time evaluation of weather conditions and experimental decision-making.

6.4 Antenna Measurements

We have planned for extensive antenna measurements and adjustments, using a remote transmitter at Nobscot Hill. This year, we plan to install there a new antenna that can be rotated about its symmetry axis to vary the transmitted linear polarization arbitrarily. The new remote transmitting antenna will enable us to specify completely the linear polarization characteristics of the radar antenna. Adjustments of the feed horn and the subreflector can be made to optimize the radar antenna performance.

The results of these measurements can be verified by backscatter measurements in light rain at vertical incidence.¹⁰ If the raindrops are randomly oriented, then the cross-covariance amplitude ratio (the cross-covariance normalized by the "main" backscattered power) approaches the value of twice the mean error amplitude $\bar{\epsilon}$. If the drops are of circular aspect, then the depolarization ratio approaches the value of four times the mean squared error $\bar{\epsilon}^2$. Rotation of the antenna in azimuth during such observations will verify the absence of any residual shape or orientation effects in the backscatter medium or reveal any azimuth dependence of the error quantities. Practically speaking, the testing of the radar system will be an on-going process, as it will be desirable to evaluate long-term changes in performance due, for example, to seasonal or diurnal environmental effects and long-term reliability of components.

10. McCormick, G. C. (1981) Polarization errors in a two-channel system, Radio Sci. 16:67-75.

References

1. Bishop, A.W., and Armstrong, G.M. (1982) A 10 cm Dual Frequency Doppler Weather Radar, Part I: The Radar System, AFGL-TR-82-0321 (I), AD A125885.
2. Ussailis, J.S., Leiker, L.A., Goodman, R.M., IV, and Metcalf, J.I. (1982) Analysis of a Polarization Diversity Weather Radar Design, AFGL-TR-82-0234, AD A121666.
3. Armstrong, G.M., and Metcalf, J.I. (1983) A Polarization Diversity Radar Data Processor, AFGL-TR-83-0111, AD A134011.
4. Bishop, A. W., and Metcalf, J.I. (1985) A Multi-Channel Radar Receiver, AFGL-TR-85-0006, AD A156058.
5. Ussailis, J.S., and Bassett, H.L. (1984) Polarization Diversity Addition to the 10 Centimeter Doppler Weather Radar, AFGL-TR-84-0239, AD A156062.
6. Bringi, V.N., Seliga, T.A., and Cherry, S.M. (1983) Statistical properties of the dual-polarization differential reflectivity (Z_{DR}) radar signal, IEEE Trans. Geosci. and Remote Sens. GE-21:215-220.
7. Offutt, W.B. (1955) A review of circular polarization as a means of precipitation clutter suppression and examples, Proc. Natl. Electron. Conf. 11:94-100.
8. Newell, R.E., Geotis, S.G., and Fleisher, A. (1957) The Shape of Rain and Snow at Microwavelengths, Res. Rept. 28, Dept. of Meteorology, Mass. Inst. of Tech.
9. Srivastava, R.C., Jameson, A.R., and Hildebrand, P.H. (1979) Time-domain computation of mean and variance of Doppler spectra, J. Appl. Meteorol. 18:189-194.
10. McCormick, G.C. (1981) Polarization errors in a two-channel system, Radio Sci. 16:67-75.

END

DATE

3-88

DTIC